American Mineralogist, Volume 96, pages 1760–1767, 2011

Structural study of the coherent dehydration of wadsleyite

Yu Ye,[1,*] Joseph R. Smyth,[2] and Daniel J. Frost[3]

[1]Department of Physics, University of Colorado, Boulder, Colorado 80309, U.S.A.
[2]Department of Geological Sciences, University of Colorado, Boulder, Colorado 80309, U.S.A.
[3]Bayerisches Geoinstitut, Universität Bayreuth, Bayreuth, D95440, Germany

Abstract

The coherent dehydration of pure-Mg wadsleyite has been investigated by single-crystal X-ray diffraction at high temperature and room pressure. Hydrous wadsleyite with 2.8 wt% H_2O has monoclinic unit-cell parameters of a = 5.6693(4), b = 11.571(1), c = 8.2407(5) Å, β = 90.209(3)°, and V = 540.59(7) Å^3. Dehydration begins at 635 K with an abrupt increase in the a-axis and decrease in b. After dehydration is complete, the dehydrated sample is orthorhombic with a = 5.6995(3), b = 11.4589(8), c = 8.2556(5) Å, and V = 539.17(6) Å^3 at ambient conditions. Atom position and displacement parameters have been refined for both hydrous and dehydrated wadsleyite samples from intensity measurements conducted at high temperatures. The most significant changes during dehydration are systematic decreases in M2–O1 and M3–O1 bond lengths. After dehydration, M2–O1 and M3–O1 bonds decrease by 3% and 2.5%, respectively. While the length changes of the other M–O bonds are no more than 1%, consistent with the hydration mechanism being protonation of O1. For the monoclinic structure, the average thermal expansion coefficient is 38.4(3) × 10^{-6} K^{-1} before dehydration and 28.1(8) × 10^{-6} K^{-1} for the dehydrated sample. The volumetric thermal expansion coefficients for MgO_6 octahedra in the hydrous sample, $\alpha_0(V)$, are 36(4), 41(4), 49(5), and 35(4) (10^{-6} K^{-1}) for M1, M2, M3A, and M3B, respectively. In the dehydrated sample, they are 35(5), 34(4), and 36(2) (10^{-6} K^{-1}) for M1, M2, and M3, respectively. No significant thermal expansion is observed for SiO_4 tetrahedra of either the hydrous or dehydrated sample.

Keywords: Hydrous, dehydrated, wadsleyite, thermal expansion

Introduction

For a pyrolite-composition mantle (Anderson 2007; Ringwood 1966), wadsleyite composes 60~70 vol% of the upper transition zone (410–525 km). At 410 km depth, olivine transforms to wadsleyite (P ≈ 13.5 GPa, T ≈ 1673 K), and at 525 km depth, wadsleyite transforms to ringwoodite (P ≈ 17.5 GPa, T ≈ 1790 K). Holl et al. (2008) and Ye et al. (2010) outlined the systematic decrease in isothermal bulk modulus (i.e., increasing in compressibility) with hydration of wadsleyite. Ye et al. (2009) reported an increased thermal expansion coefficient for hydrous wadsleyite of 1.66 wt% H_2O relative to that for anhydrous wadsleyite. To confirm this result and see if the increased thermal expansion extends systematically to higher water contents, we have measured the thermal expansion of a more hydrous wadsleyite sample with 2.8 wt% H_2O.

Smyth et al. (1997), Kudoh and Inoue (1999), Holl et al. (2008), and Ye et al. (2010) outlined the monoclinic ($I2/m$) structure of hydrous wadsleyite with β slightly greater than 90°, due to non-equivalent vacancy ordering in the M3 octahedra that split into two separate sites in the monoclinic structure. In this study, we measure the β angle of hydrous wadsleyite at various temperatures and during the dehydration process, and explore the relationship between the β angle and M3 occupancies and polyhedral volumes.

Smyth (1987, 1994) predicted that wadsleyite could contain up to 3.3 wt% H_2O, because non-silicate O1 sites are likely sites for protonation. This structure prediction was further supported by the ^{29}Si NMR spectroscopic study of Stebbins et al. (2009a 2009b). To document structural effects of dehydration, especially for M2–O1 and M3–O1 bonds, crystal-structure refinements have been carried out at high temperatures for both hydrous and dehydrated samples.

Experimental methods and data

Synthesis conditions for the hydrous wadsleyite sample were 15 GPa and 1523 K (Ye et al. 2010). A single crystal of about 110 × 80 × 70 μm^3 in size was mounted inside a silica glass capillary for unit-cell and internal structure refinement. Experiments were conducted on a Bruker P4 four-circle diffractometer with a dual scintillation point detector system using an 18 kW rotating Mo-anode X-ray generator operated at voltage of 50 kV and current of 250 mA. The X-ray source was Mo$K\alpha_1$–Mo$K\alpha_2$ mixed characteristic wavelength, and a single crystal of anhydrous forsterite with perfect spherical shape was used to calibrate Mo$K\alpha$(average) to be 0.71065 Å, which was later used for the cell and structure refinement of the wadsleyite sample. The initial unit-cell parameters at room temperature were refined from 70 single-crystal reflections of 21 unique reflections (12° < 2θ < 30°):

* E-mail: yey@colorado.edu

a = 5.6683(12), b = 11.571(3), c = 8.2412(16) Å, and V = 540.46(19) Å^3 for the orthorhombic (*Imma*) structure; a = 5.6693(4), b = 11.571(1), c = 8.2407(5) Å, β = 90.209(3)°, and V = 540.59(7) Å^3 for the monoclinic structure with space group *I*2/*m*. The refined monoclinic unit-cell parameters have smaller errors than the orthorhombic, hence, in the following discussion we adopt monoclinic structure for the hydrous wadsleyite. In addition, Ye et al. (2010) reported the monoclinic unit-cell parameters of another single crystal but from the same sample source as: a = 5.6686(8), b = 11.569(1), c = 8.2449(5) Å, β = 90.14(1)°, and V = 540.7(1) Å^3. Also, Holl et al. (2008) reported β angles ranging from 90.09 to 90.16° for hydrous wadsleyite samples of 1.66 wt% H_2O. The unit-cell parameters from Ye et al. (2010) (identical sample source) showed about a 0.004 Å larger c-axis, and about a 0.07° smaller β angle, compared with those of this study, while a, b, and V are quite consistent with the current values. Since the b/a ratio of the current sample is the same as that of Ye et al. (2010), we assume that the water content in the current study is also 2.8(5) wt% (Jacobsen et al. 2005), indicating a chemical formula of $Mg_{1.79}H_{0.42}SiO_4$ for the present hydrous wadsleyite sample. Intensity measurements were carried out on a point-detector diffractometer with about one thousand reflections and 2θ up to 65° (Table 1).

A Bruker high-temperature device was mounted on the diffractometer for high-temperature measurements. The device used two-prong ceramic-coated Pt wire radiant heating with an Omega temperature-control unit, and the crystal was centered between the two prongs. The temperature calibration was described in detail by Ye et al. (2009). Nine high-temperature measurements with intervals of about 50 K were taken up to 736 K. For each temperature step, the process at initial ambient condition for unit-cell and internal structure refinements was repeated, except that we decreased the 2θ scan range to 60°, as the prongs were found to block some reflections at high 2θ angles. For measurements at 586 and 635 K, the internal structure became somewhat defective and disordered due to dehydration, the reflection peaks become about 50% broader in ω scans. Most of the reflections at large 2θ angle became very weak so we reduced the 2θ scan range to 55°. In addition, we were unable to conduct intensity scans at the highest temperature (736 K), because of temperature instability over the data collection period.

After heating to 736 K, unit-cell parameters at room temperature were a = 5.6995(3), b = 11.4589(8), c = 8.2556(5) Å, and V = 539.17(6) Å^3 for the orthorhombic structure; a = 5.6994(4), b = 11.4567(9), c = 8.2546(6) Å, β = 90.014(1)°, and V = 538.94(6) Å^3 for the monoclinic structure. The β-angle decreased by about 0.2° compared with the initial cell, and the diffraction peaks became sharp again. There was no significant difference between the parameters of the orthorhombic and monoclinic unit cells for the dehydrated sample, and both gave b/a ratios of 2.010, indicating that the water content of the dehydrated crystal was 0.16 wt%. Hence, we conclude that the hydrous sample lost nearly all water by 736 K, and the dehydrated sample was a sufficiently good crystal for further measurement to facilitate comparison with the hydrous sample. After dehydration, the crystal was treated as orthorhombic (*Imma*). For the dehydrated sample, we repeated the experiment process with unit-cell parameter refinements up to 767 K, and intensity scans up to 705 K. Fewer reflections were measured for each intensity scan in the higher symmetric space group than that of the monoclinic structure.

The refined unit-cell parameters and intensity collection parameters for the hydrous and dehydrated samples are listed in Tables 1 and 2, respectively. The intensity data are used for refinements of atom position coordinates, occupancies, and anisotropic displacement parameters using the program SHELXL-97 (Sheldrick 1997) within the software package WinGX (Farrugia 1999). The scattering factors of Mg^{2+} and Si^{4+} adopted are from Cromer and Mann (1968), and those of O^{2-} are reported by Tokonami (1965). For the *I*2/*m* structure, some of the atomic coordinates are fixed: for M1 $x = y = z = 0$; for M2 $y = ¼$; for M3A $x = z = ¼$; for M3B $x = ¾$, $z = ¼$; for O1 and O2 $y = ¼$. The refined atomic position coordinates for hydrous and dehydrated samples are listed in Tables 3 and 4. The occupancies of O^{2-} ions are fixed to 1 (full), whereas cation occupancies should be no greater than 1 due to H^+ substitution. The refined cation occupancies for hydrous and dehydrated samples are listed in Table 5. The occupancies for hydrous sample at room temperature give an estimated Mg/Si ratio of 1.84(2), while the chemical formula gives a ratio of 1.79, assuming full occupancy for Si. The crystal structures were refined using anisotropic displacement parameters, but to simplify the discussion, we only listed the equivalent displacement parameters for hydrous and dehydrated samples in Appendices 1[1] and 2[1]. Based on the atomic position coordinates, bond lengths and polyhedral volumes were calculated by the software package XTALDRAW (Downs et al. 1993) for both hydrous and dehydrated samples, which are listed in Appendices 3[1] and 4[1].

Results and discussion

Unit-cell parameters

The unit-cell parameters are plotted vs. temperature for the hydrous and dehydrated samples in Figures 1a–1d, together with those of hydrous (1.66 wt% H_2O) and anhydrous wadsleyite samples from Ye et al. (2009) for comparison. Dehydration of the current sample began around 635 K, as seen by the abnormal increase in a and the decrease in b around 635 K, consistent with dehydration observations by Inoue et al. (2004) and Ye et al. (2009). Ye et al. (2009) reported the beginning of dehydration around 655 K for the sample with 1.66% H_2O. For both hydrous samples, the c axes increase only slightly around the start of dehydration, however they increase significantly after onset of

[1] Deposit item AM-11-062, Appendix Tables. Deposit items are available two ways: For a paper copy contact the Business Office of the Mineralogical Society of America (see inside front cover of recent issue) for price information. For an electronic copy visit the MSA web site at http://www.minsocam.org, go to the *American Mineralogist* Contents, find the table of contents for the specific volume/issue wanted, and then click on the deposit link there.

Table 1. Unit-cell parameters and data collection parameters for hydrous sample [space group: *I*2/*m* with origin shift (¼, ¼, ¼)]

T (K)	303	350	396	443	489	537	586	635	685	736
a (Å)	5.6693(4)	5.6711(5)	5.6725(4)	5.6753(4)	5.6779(4)	5.6795(5)	5.6827(6)	5.6897(7)	5.7120(5)	5.7190(4)
b (Å)	11.571(1)	11.575(1)	11.580(1)	11.586(1)	11.595(1)	11.607(1)	11.616(1)	11.615(2)	11.509(1)	11.494(1)
c (Å)	8.2407(5)	8.2451(8)	8.2500(6)	8.2564(7)	8.2648(7)	8.2735(8)	8.2749(8)	8.283(1)	8.2931(7)	8.3008(5)
β (°)	90.209(3)	90.208(5)	90.207(5)	90.223(5)	90.267(5)	90.473(5)	90.448(6)	90.268(7)	90.019(5)	90.018(2)
V (Å^3)	540.59(7)	541.21(9)	541.90(8)	542.89(8)	544.10(9)	545.40(9)	546.23(9)	547.4(1)	545.21(8)	545.61(5)
No. unique Total	951	805	802	804	801	780	628	636	792	
No. unique $I > 4\sigma$	702	640	626	630	625	529	405	397	613	
GooF	1.334	1.580	1.561	1.718	1.776	1.783	2.524	2.324	1.783	
R_1 for $I > 4\sigma$ (%)	4.03	4.20	4.22	4.68	5.16	6.79	10.51	10.11	5.89	
R_{int} (%)	1.79	2.71	1.60	2.16	1.70	3.90	4.02	4.76	9.78	

Table 2. Unit-cell parameters and data collection parameters for dehydrated sample (space group: *Imma*)

T (K)	303	359	415	471	527	586	645	705	767
a (Å)	5.6995(3)	5.7015(3)	5.7037(4)	5.7063(5)	5.7083(3)	5.7105(3)	5.7141(4)	5.7180(4)	5.7205(4)
b (Å)	11.4589(8)	11.4613(8)	11.4664(8)	11.4706(13)	11.4749(8)	11.4798(8)	11.4845(8)	11.4915(11)	11.4960(9)
c (Å)	8.2556(5)	8.2609(5)	8.2662(5)	8.2718(8)	8.2776(5)	8.2826(5)	8.2912(5)	8.2984(7)	8.3043(6)
V (Å3)	539.17(6)	539.82(6)	540.62(6)	541.42(9)	542.20(6)	542.97(6)	544.09(6)	545.27(8)	546.16(6)
No. unique Total	430	433	439	434	433	439	435	434	
No. unique $I > 4\sigma$	373	374	376	358	362	374	367	364	
GooF	1.835	1.658	1.711	1.596	1.635	1.612	1.705	1.529	
R_1 for $I > 4\sigma$ (%)	4.55	4.60	4.55	4.20	4.27	4.70	4.66	4.21	
R_{int} (%)	2.98	6.90	6.64	6.21	6.14	6.63	5.51	7.44	

TABLE 3. Refined atomic position coordinates for hydrous sample

T (K)		303	350	396	443	489	537	586	635	685
M2:	*x*	0.0006(2)	0.0007(2)	0.0007(2)	0.0006(3)	0.0010(3)	0.0025(4)	0.0015(9)	0.0004(9)	−0.0002(3)
	z	0.9708(1)	0.9708(1)	0.9708(1)	0.9706(1)	0.9708(2)	0.9706(3)	0.9709(5)	0.9698(5)	0.9694(2)
M3A:	*y*	0.1203(1)	0.1205(1)	0.1203(1)	0.1205(1)	0.1207(2)	0.1202(3)	0.1198(5)	0.1225(5)	0.1273(1)
M3B:	*y*	0.3796(1)	0.3796(1)	0.3796(1)	0.3795(1)	0.3795(1)	0.3798(2)	0.3799(5)	0.3776(5)	0.3729(1)
Si:	*x*	0.0002(1)	0.0000(1)	−0.0001(1)	0.0000(1)	0.0000(1)	−0.0003(2)	−0.0001(5)	0.0002(5)	0.0000(1)
	y	0.12120(5)	0.12107(6)	0.12115(5)	0.12122(6)	0.12127(7)	0.1215(1)	0.1215(2)	0.1211(2)	0.11988(8)
	z	0.61541(6)	0.61538(7)	0.61528(7)	0.61534(8)	0.61531(9)	0.6150(1)	0.6151(2)	0.6158(2)	0.6168(1)
O1:	*x*	−0.0004(4)	−0.0003(5)	−0.0002(5)	−0.0003(5)	−0.0004(6)	−0.0003(8)	0.001(2)	0.002(2)	−0.0001(6)
	z	0.2265(3)	0.2267(3)	0.2266(3)	0.2262(4)	0.2257(4)	0.2255(5)	0.225(1)	0.221(1)	0.2171(5)
O2:	*x*	−0.0005(4)	0.0001(5)	−0.0009(5)	0.0002(6)	−0.0007(6)	−0.0010(8)	−0.000(2)	−0.001(2)	−0.0004(6)
	z	0.7164(2)	0.7159(3)	0.7159(3)	0.7159(3)	0.7156(3)	0.7144(5)	0.714(1)	0.715(1)	0.7156(4)
O3:	*x*	−0.0005(3)	0.0000(3)	−0.0003(3)	−0.0008(4)	−0.0003(4)	−0.0008(6)	0.001(1)	−0.001(1)	0.0001(4)
	y	0.9865(1)	0.9866(1)	0.9867(1)	0.9866(2)	0.9864(2)	0.9858(3)	0.9860(5)	0.9866(5)	0.9894(2)
	z	0.2564(2)	0.2567(2)	0.2567(2)	0.2567(2)	0.2565(2)	0.2568(4)	0.2563(6)	0.2570(7)	0.2563(3)
O4A:	*x*	0.2598(3)	0.2602(3)	0.2601(3)	0.2603(3)	0.2603(4)	0.2611(5)	0.259(1)	0.261(1)	0.2623(4)
	y	0.1243(1)	0.1242(1)	0.1242(1)	0.1241(1)	0.1241(2)	0.1250(3)	0.1249(5)	0.1242(2)	0.1225(2)
	z	0.9951(2)	0.9949(2)	0.9948(2)	0.9948(2)	0.9945(2)	0.9946(3)	0.9949(6)	0.9940(6)	0.9924(3)
O4B:	*x*	0.7410(3)	0.7410(3)	0.7408(3)	0.7409(3)	0.7411(4)	0.7418(5)	0.742(1)	0.740(1)	0.7387(4)
	y	0.3762(1)	0.3761(1)	0.3761(1)	0.3760(1)	0.3791(2)	0.3757(3)	0.3749(5)	0.3756(6)	0.3774(2)
	z	0.9955(2)	0.9958(2)	0.9956(2)	0.9956(2)	0.9956(2)	0.9962(3)	0.9964(5)	0.9948(6)	0.9921(3)

TABLE 4. Refined atomic position coordinates for dehydrated sample

T (K)		303	359	415	471	527	586	645	705
M2:	*z*	0.9705(2)	0.9703(2)	0.9702(2)	0.9699(2)	0.9698(2)	0.9698(2)	0.9696(2)	0.9694(2)
M3:	*y*	0.1272(1)	0.1271(1)	0.1271(1)	0.1272(1)	0.1271(1)	0.1272(1)	0.1270(1)	0.1271(1)
Si:	*y*	0.1199(1)	0.1198(1)	0.1199(1)	0.1199(1)	0.1200(1)	0.1198(1)	0.1199(1)	0.1198(1)
	z	0.6167(1)	0.6167(1)	0.6167(1)	0.6167(1)	0.6166(1)	0.6167(1)	0.6166(1)	0.6167(1)
O1:	*z*	0.2184(5)	0.2179(5)	0.2174(5)	0.2179(5)	0.2178(5)	0.2178(5)	0.2180(5)	0.2170(5)
O2:	*z*	0.7168(5)	0.7172(5)	0.7167(5)	0.7169(4)	0.7166(4)	0.7169(5)	0.7165(5)	0.7160(4)
O3:	*y*	0.9897(2)	0.9897(2)	0.9895(2)	0.9895(2)	0.9897(2)	0.9896(2)	0.9896(2)	0.9892(2)
	z	0.2555(3)	0.2557(3)	0.2559(3)	0.2557(3)	0.2559(3)	0.2558(3)	0.2555(3)	0.2559(3)
O4:	*x*	0.2613(3)	0.2610(3)	0.2618(3)	0.2622(3)	0.2619(3)	0.2614(3)	0.2616(3)	0.2622(3)
	y	0.1226(1)	0.1227(1)	0.1227(1)	0.1227(1)	0.1228(1)	0.1227(1)	0.1226(1)	0.1227(1)
	z	0.9924(2)	0.9926(2)	0.9924(2)	0.9926(2)	0.9922(2)	0.9922(2)	0.9922(2)	0.9920(2)

TABLE 5. Cation occupancy factors for both hydrous and dehydrated samples

Hydrous						Dehydrated				
T (K)	M1	M2	M3A	M3B	Si	*T* (K)	M1	M2	M3	Si
303	1.00(1)	1.00(1)	0.773(6)	0.819(6)	0.968(5)	303	0.93(1)	0.93(1)	0.92(1)	0.94(1)
350	1.00(1)	1.00(1)	0.785(8)	0.832(8)	0.964(7)	359	1.00(1)	1.00(1)	0.986(8)	0.99(1)
396	1.00(1)	1.00(1)	0.788(8)	0.830(8)	0.960(6)	415	0.989(9)	0.995(9)	0.982(8)	1.00(1)
443	1.00(1)	1.00(1)	0.788(8)	0.845(9)	0.968(7)	471	0.987(8)	1.00(1)	0.979(8)	1.00(1)
489	1.00(1)	1.00(1)	0.772(9)	0.833(9)	0.965(8)	527	0.93(2)	0.95(2)	0.93(2)	0.95(2)
537	1.00(1)	0.98(1)	0.72(1)	0.84(1)	0.944(9)	586	1.00(1)	1.00(1)	0.990(8)	0.99(1)
586	0.98(4)	0.95(3)	0.73(3)	0.73(3)	0.92(3)	645	0.95(2)	0.95(2)	0.93(2)	0.96(2)
635	0.97(2)	1.00(2)	0.79(2)	0.82(2)	0.98(2)	705	0.96(2)	0.96(2)	0.95(2)	0.98(2)
685	1.00(1)	1.00(1)	1.00(1)	1.00(1)	1.00(1)					

dehydration. For hydrous samples there are "steps" on the *c*-*T* plots in the vicinity of the start-point of dehydration. The *c* axis of this study's hydrous sample increased by 0.0088(8) Å from 489 to 537 K, 0.0014(10) Å from 537 to 586 K, and 0.0082(9) Å from 586 to 635 K, the "step" being from 537 to 586 K, just before dehydration. The *c* axis of the hydrous sample from Ye et al. (2009) showed an increase of 0.0065(8) Å from 508 to 557 K, 0.0021(10) Å from 557 to 606 K, 0.0015(9) Å from 606 to 655 K, and 0.0081(9) Å from 655 to 705 K: the "step" here is from 557 to 655 K, before and after the starting point of dehydration. In addition, the temperature intervals for Ye et al. (2009) were also about 50 K. After dehydration, the unit-cell parameters at ambient condition showed 0.53 and 0.18% increases in the *a* and *c* axes, respectively, and a 0.97 and 0.26% decrease in *b* axis and *V*, respectively. This is consistent with the relationship of unit-cell parameters to water content (Holl et al. 2008).

The average axial and volume thermal expansion coefficients (α_0) for each sample are listed in Table 6. For hydrous samples, α_0 values are calculated before dehydration. α_b, α_c, and α_V show a significant systematic increase with water contents. Holl et al. (2008) and Ye et al. (2010) reported that the mean isothermal axial and bulk compressibilities β_a, β_b, β_c, and β_V values of wadsleyite also systematically increase with water contents. This is also consistent with a systematic decrease in adiabatic bulk modulus, K_{S0}, shear modulus G_0, and longitudinal components of moduli C_{11}, C_{22}, and C_{33} as water content increases (Mao et al. 2008a). In addition, for each sample, α_c is greater than α_a and α_b, which is also consistent with the order of axial compressibilities for wadsleyite (Holl et al. 2008; Ye et al. 2010).

The thermal expansion coefficient is defined as:

$$\alpha = 1/V(\partial V/\partial T)_p = (\partial \ln V/\partial T)_p. \quad (1)$$

The data points in Figures 1a–1d fit well to a second-order polynomial function (for hydrous samples fitting curves are just before dehydration). The dehydrated sample in the current study has almost the same *a*−*T* and *V*−*T* data sets as those of the anhydrous sample in Ye et al. (2009), but a slightly larger *b*−*T*

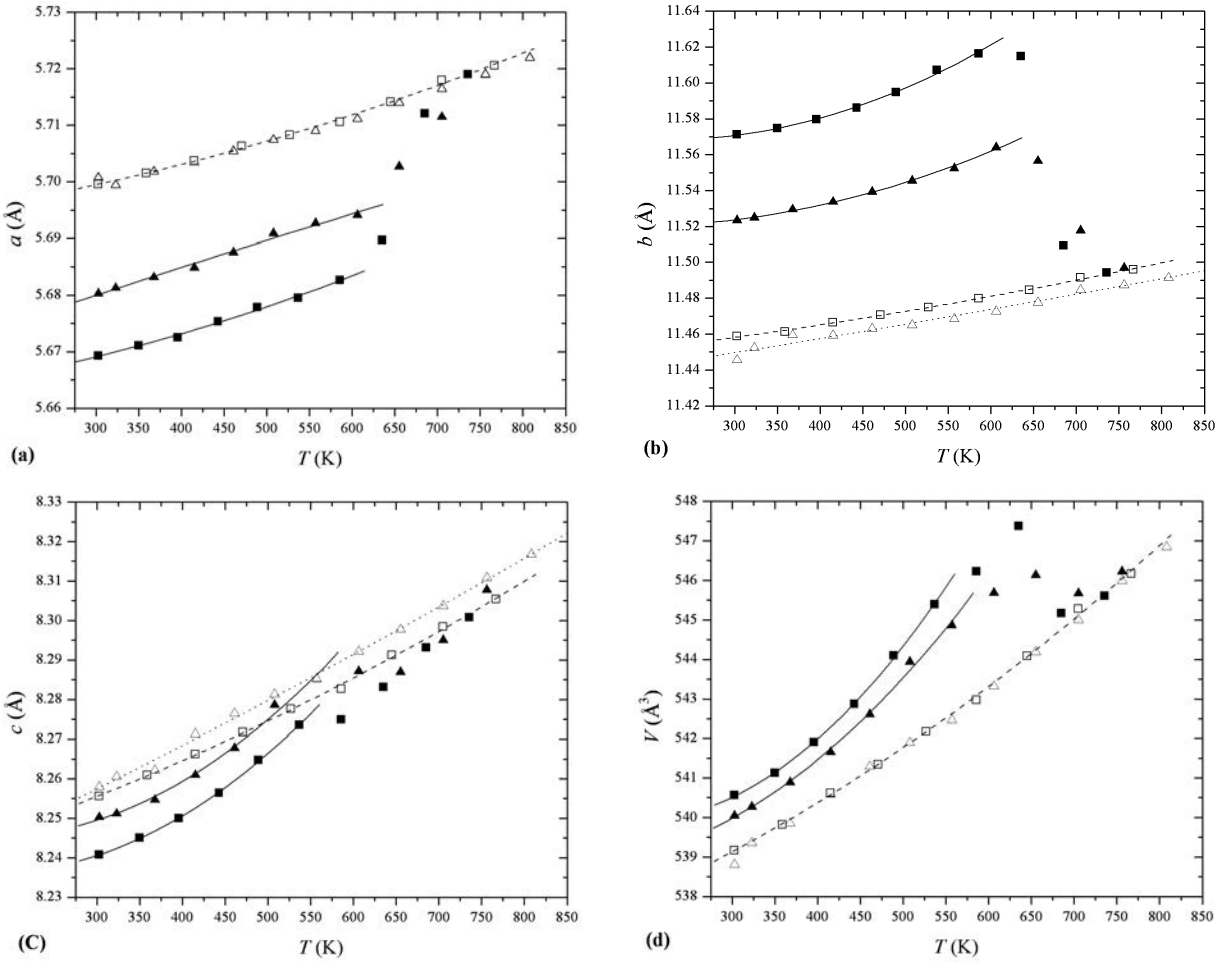

FIGURE 1. (**a**–**d**) Unit-cell parameters of *a*, *b*, *c*, and *V* vs. temperature *T*, respectively. Solid and open square symbols stand for hydrous and dehydrated sample of this study, respectively; while solid and open triangle symbols stand for hydrous and anhydrous wadsleyite from Ye et al. (2009), respectively. The solid curves are second-order polynomial fitting for both the hydrous wadsleyite samples before dehydration; the dash curves are second-order polynomial fitting for the dehydrated sample of this study, throughout the experimental temperature range, and in **b** and **c** the dot curves of second-order polynomial are for anhydrous sample of Ye et al. (2009).

TABLE 6. Average thermal expansion coefficients (α_0 10^{-6} K) of axes and volume for hydrous and anhydrous wadsleyite samples

	$\alpha_0(a)$	$\alpha_0(b)$	$\alpha_0(c)$	$\alpha_0(V)$	*T* range	
anhydrous	7.6(3)	7.1(3)	14.0(3)	28.5(5)	303–808 K	Ye et al. (2009)
dehydrated	8.0(3)	7.1(2)	12.9(3)	28.1(8)	303–767 K	This study
1.66 wt% H_2O	8.4(3)	11.0(7)	16.4(10)	35.8(14)	303–606 K	Ye et al. (2009)
2.8 wt% H_2O	8.0(4)	13.1(1)	17.0(1)	38.4(3)	303–586 K	This study

file and a slightly smaller *c*−*T* file. Hence, the anhydrous sample in Ye et al. (2009) shares the same fitting curves with the current dehydrated sample in Figures 1a–1d, but are fitted separately in Figures 1b and 1c. The second-order polynomial fitting indicates that the axial and volume thermal expansion coefficients can also be expressed as linear temperature dependence of:

$$\alpha = a_1 \times T + a_0. \quad (2)$$

The axial and volume a_1/a_0 values of each sample are listed in Table 7. Some of the a_0 values for hydrous samples are negative, because the data are fit above room temperature, ignoring the unit-cell parameters at lower temperatures. a_1 values generally increase as the water content increasing, which means that hydration has larger contribution to the thermal expansion at higher temperature.

Crystal structure

The β-angle of the hydrous sample remained at about 90.2° up to 489 K (Table 1). At 537 and 586 K, β increased significantly to more than 90.4°, however, the residual refinement value R1 also increased to more than 10% at 586 K, indicating that the crystal structure became somewhat disordered, which induced larger uncertainties for the refined atomic position coordinates,

TABLE 7. $a_1\ 10^{-8}\ K^{-2}$ and $a_0\ 10^{-4}\ K^{-1}$ for temperature-dependent thermal expansion coefficients of axes and volume, as indicated in Equation 2, for hydrous and anhydrous wadsleyite with the same temperature range

		a	*b*	*c*	*V*
Anhydrous	a_1	0.7(1)	0.9(2)	0.4(1)	2.4(4)
	a_0	0.042(9)	0.02(1)	0.12(2)	0.15(2)
Dehydrated	a_1	0.9(2)	0.6(2)	1.1(2)	2.8(6)
	a_0	0.030(1)	0.040(1)	0.07(1)	0.13(3)
1.66 wt% H_2O	a_1	1.2(5)	4.0(6)	6.8(8)	5.0(8)
	a_0	0.03(1)	–0.07(2)	–0.12(5)	0.13(6)
2.8 wt% H_2O	a_1	1.0(7)	8.2(6)	7.9(5)	16(1)
	a_0	0.036(6)	–0.22(3)	–0.12(2)	–0.28(5)

TABLE 8. Contrast and comparison of M3 sites occupancies, polyhedral volumes, and β for several hydrous wadsleyite samples

Water content (wt%)	1.66*	1.8†	2.3‡	2.8§	2.8‖	3.3†
M3A occup. (%)	87.1(2)	88(2)	83(2)	80.5(4)	77.3(6)	76(2)
Poly. *V* (Å^3)	12.096(8)	12.02(1)	12.17(1)	12.110(1)	12.14(1)	12.19(1)
M3B occup. (%)	85.7(2)	84(1)	90(2)	80.3(3)	81.9(6)	76(1)
Poly. *V* (Å^3)	12.123(8)	12.07(1)	12.02(1)	12.100(1)	12.08(1)	12.21(1)
V difference (Å^3)	0.027(8)	0.05(1)	0.15(1)	0.010(1)	0.06(1)	0.02(1)
β (°)	90.09(1)	90.21(1)	90.40(1)	90.14(1)	90.209(3)	90.09(4)

* Holl et al. (2008).
† Kudoh and Inoue (1999).
‡ Joseph et al. (1997) of Fo_{95}, while other samples are Fo_{100}.
§ Ye et a. (2010).
‖ This study.

occupancies, and displacement parameters. At 685 K, dehydration was almost complete and β decreased to 90.02°, R_1 decreased to 5.89%, and reflection peaks became sharp again.

According to Deon et al. (2010), M3 sites are preferable cation sites for H^+ substitution, and the calculated occupancy should be 0.79 for the current hydrous Fo_{100} wadsleyite with 2.8 wt% H_2O. In Table 5, M1, M2, and Si sites remained fully occupied throughout the temperature range for the hydrous sample, and the occupancies of M3A and M3B ranged mostly 0.73~0.79 and 0.82~0.85, respectively, till 635 K, whereas at 685 K, these occupancies increased to 1.00 after dehydration. For the dehydrated sample, the occupancies of the M3 site were close to 1 at various temperatures, similar as those of the other cation sites. These results also imply that the Mg/Si ratio in the wadsleyite phase might increase after dehydration, possibly nucleating a second phase of lower Mg/Si ratio such as pyroxene, quartz, or stishovite. However, the diffraction images for the dehydrated sample from the Bruker CCD area detector showed no extra reflections or powder diffraction rings that might indicate the presence of other crystalline phases. All the reflection spots could be indexed well as single-crystal reflections from the wadsleyite phase. Hence, the presence of other crystalline phases could not be detected by the experimental method of X-ray diffraction here.

The β angles, M3 occupancies and polyhedral volumes for several hydrous wadsleyite samples (monoclinic structure) are listed in Table 8. The sample from Ye et al. (2010) was from the same capsule source as the current sample with identical water content, but had a smaller β angle, which could be attributed to the smaller difference between M3A and M3B volumes from Ye et al. (2010). Also, there was no significant difference between the occupancies of M3A and M3B for the sample from Ye et al. (2010). Table 8 shows the general trend that a larger difference between occupancies of M3A and M3B sites induces a larger difference between non-equivalent M3 volumes, and as a result, β increases. This experimental evidence supports the hypothesis that non-equivalent distribution of vacancies at M3A and M3B sites is correlated with the decrease of symmetry of hydrous wadsleyite as a function of hydrogen content, upon quenching (Kudoh and Inoue 1999; Holl et al. 2008; Smyth et al. 1997). In addition, in identical samples, non-equivalent M3 sites generally have larger polyhedral volumes and smaller occupancies, i.e., more H^+ substitution regardless of whether it is M3A or M3B.

For both hydrous and dehydrated samples, the calculated Mg–O bond lengths are plotted vs. temperature in Figures 2a–2d. The most significant changes after dehydration are that M2–O1 and M3–O1 bonds decrease by 3 and 2.5%, respectively, as indicated by Figure 2a, where M2–O1 and M3–O1 bonds are connected by solid and dotted lines, respectively. For other M–O bonds after dehydration: M1–O3 and M1–O4 bonds decrease by 0.2%, respectively (Fig. 2b); M2–O4 bonds increase by 0.7%, and M2–O3 decrease by 0.4% (Fig. 2c); and M3–O3 and M3–O4 bonds increase by 1%, respectively (Fig. 2d). Nonsilicate O1 atoms are sites of protonation (Smyth 1987, 1994), and Holl et al. (2008) also reported a significant and systematic increase in M2–O1 and M3–O1 bond length with increasing water content. Hence, it is reasonable for bonds around O1 to shrink after dehydration.

MgO_6 octahedral volumes are plotted vs. temperature in Figure 3. For the hydrous sample, MgO_6 octahedral volumes vs. *T* are fitted to 489 K, because of the defect structure at temperatures above 489 K. The calculated $\alpha_0(V)$ values are 36(4), 41(4), 49(5), and 35(4) ($10^{-6}\ K^{-1}$) for M1, M2, M3A, and M3B, respectively, for the hydrous sample up to 489 K; 35(5), 34(4), and 36(2) ($10^{-6}\ K^{-1}$) for M1, M2, and M3, respectively, for the dehydrated sample up to 705 K. Based on the linear fittings, *V*(M1) and *V*(M2) shrink about 1 and 0.6%, respectively, after dehydration, which is consistent with the size order of MgO_6 octahedral volumes as functions of water content, reported by Holl et al. (2008). Dehydrated *V*(M3) is about 1% smaller than *V*(M3A), but identical with *V*(M3B).

In addition, SiO_4 tetrahedral volumes vs. temperature are plotted in Figure 4 for both hydrous and dehydrated samples. They do not show significant expansion at high temperatures, due to the strong Si–O bond connection. And the dehydrated *V*(Si) is about 7% smaller than the hydrous one, a difference comparable to the uncertainties.

Implications for the 410 km discontinuity

The average thermal expansion coefficients for both anhydrous and hydrous wadsleyite are listed in Table 6. Holl et al. (2008) reported K_{T0} (isothermal bulk modulus at ambient pressure) values of 173(5) and 160(1) GPa for anhydrous and 1.66 wt% H_2O wadsleyite samples, respectively, with $K' = 4$, whereas Ye et al. (2010) report K_{T0} = 137(5) GPa, $K' = 4.5$ for hydrous wadsleyite with 2.8 wt% H_2O. The calculated ambient densities for anhydrous, 1.66 wt% H_2O, and 2.8 wt% H_2O wadsleyite samples are (g/cm^3) 3.454, 3.376 (Ye et al. 2009), and 3.328 (this study), respectively. Li et al. (1998) reported $(dK_S/dT)_P$ of -1.2×10^{-2} GPa/K for anhydrous wadsleyite, and we assume the same value for hydrous samples. In addition, Couvy et al. (2010) reported that forsterite had $\rho = 3.202$ g/cm^3, $K_{T0} = 129(3)$ GPa, $K' = 3.88$, $(dK/dT)_P = -1.1 \times 10^{-2}$ GPa/K, and Ye et al. (2009) reported an α_0 of $36.4 \times 10^{-6}\ K^{-1}$ for anhydrous forsterite.

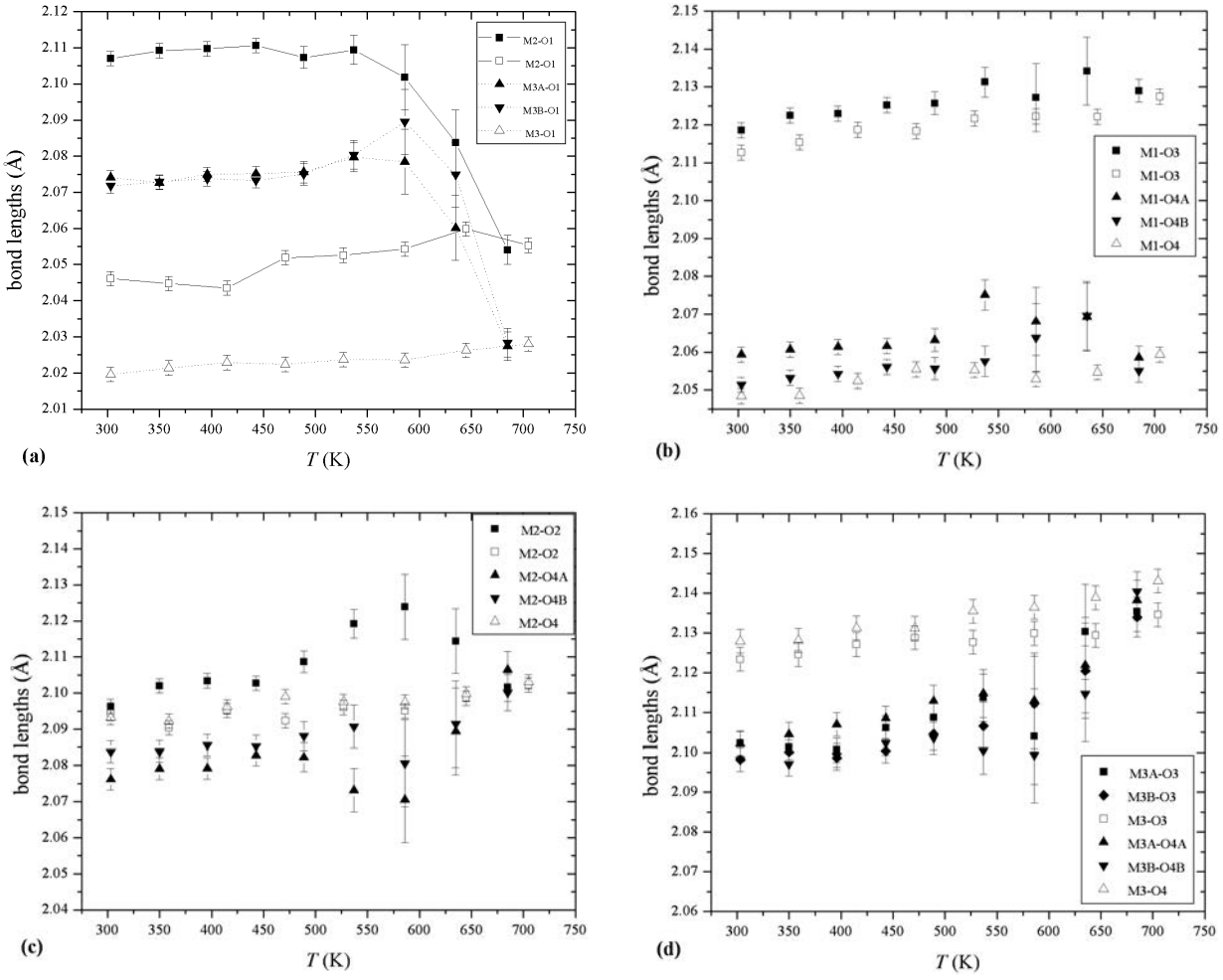

FIGURE 2. (**a**–**d**) Plots of M–O bond lengths vs. *T* of this study, with vertical error bars for the uncertainties of lengths. All solid symbols are for hydrous sample, and open symbols are for dehydrated sample.

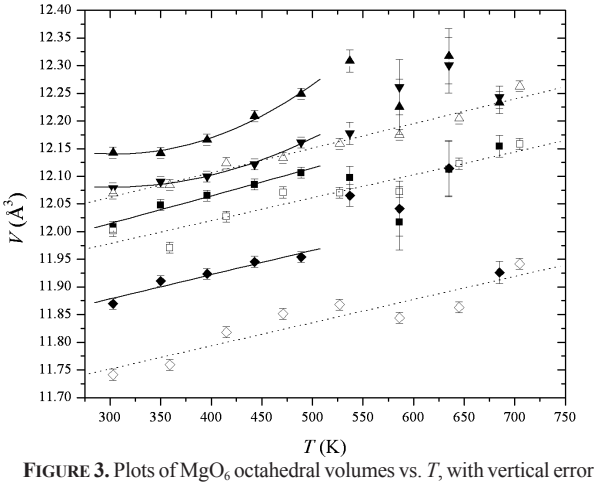

FIGURE 3. Plots of MgO_6 octahedral volumes vs. *T*, with vertical error bars for uncertainties of polyhedral volumes (diamond = M1; square = M2; up triangle = M3A or M3; down triangle = M3B). Solid symbols are for the hydrous sample with solid fitting curves (303–489 K), and open symbols are for the dehydrated sample with dot fitting lines. The fitting for M3A and M3B are second-order polynomial, while others are linear fitting.

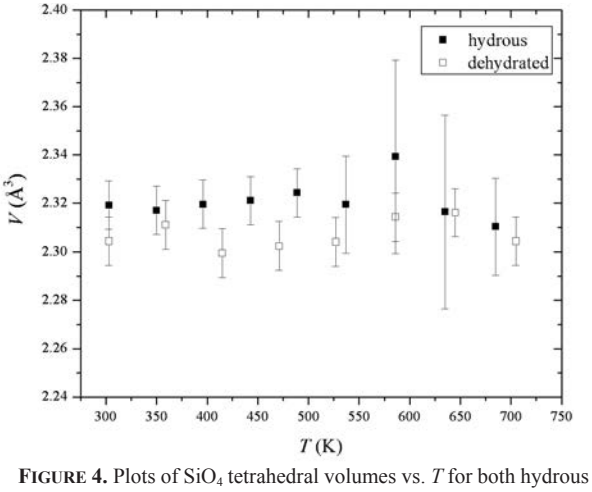

FIGURE 4. Plots of SiO_4 tetrahedral volumes vs. *T* for both hydrous and dehydrated sample of this study. The vertical error bars are for uncertainties of polyhedral volumes.

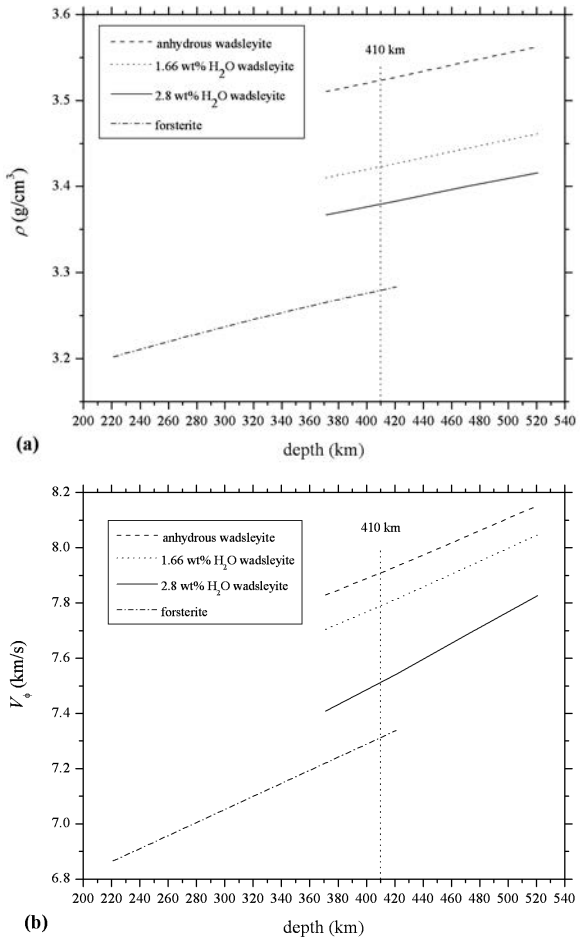

FIGURE 5. (**a** and **b**) Density and bulk sound velocity, respectively, as functions of depth in the upper mantle and transition zone for various wadsleyite and forsterite samples.

The bulk sound velocity is calculated from adiabatic bulk modulus and density in Equation 3:

$$V_\Phi(P,T) = [K_S(P,T)/\rho(P,T)]^{1/2}. \quad (3)$$

The relationship between adiabatic and isothermal bulk compressibilities is

$$K_S = K_T \times (1 + \alpha\gamma T) \quad (4)$$

whereas α and γ are thermal expansion coefficient and Grüneisen parameter (Chopelas 1991), respectively. Then, the density $\rho(P,T)$ and adiabatic bulk modulus $K_S(P,T)$ at high temperature and high pressure can be expressed in Equations 5 and 6, respectively:

$$\rho(P,T) = \rho_0 \times [1 + P/K_T - \alpha(T - T_0)] \quad (5)$$
$$K_S(P,T) = K_{S0} + (\partial K_S/\partial P)_T \times P + (\partial K_S/\partial T)_P \times (T - T_0) \quad (6)$$

where ρ_0 is the density at ambient condition, T_0 is room temperature of 300 K, and room pressure is approximated as 0 GPa.

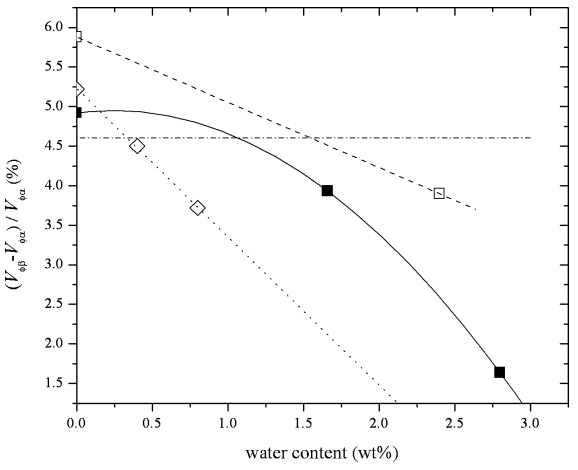

FIGURE 6. Plots of bulk sound velocity contrast at the 410 km discontinuity as a function of water content (P = 13.5 GPa and T = 1673 K). Solid square and solid fitting curve: current study; open square and dash line: Inoue et al. (2004); open diamond and dot line: Mao et al. (2008b); and the horizontal dash-dot line represent 4.6% velocity contrast.

Based on Equations 3–6, and the temperature and pressure from PREM (Dziewonski and Anderson 1981), we calculated the bulk sound velocities of olivine and wadsleyite samples of various water contents at depths in upper mantle and upper transition zone, respectively. The densities and bulk sound velocities vs. depth are plotted in Figures 5a and 5b, respectively. Since forsterite may contain water up to 0.9 wt% (Smyth et al. 2006), i.e., much less than wadsleyite, we assume anhydrous conditions for forsterite in the upper mantle and 410 km depth in this discussion. The density and bulk sound velocity profiles decrease systematically as water contents increase. Figure 5a indicates a bulk sound speed contrast $(V_{\Phi\beta} - V_{\Phi\alpha})/V_{\Phi\alpha}$ of 8.2, 6.6, and 2.7% for anhydrous, 1.66 wt% H_2O, and 2.8 wt% H_2O wadsleyite samples, respectively, at 410 km discontinuity. According to a pyrolite mantle composition model, olivine plus wadsleyite compose about 60 vol% in upper mantle and upper transition zone. Hence, the bulk velocity contrast vs. water content from the current study is plotted in Figure 6, compared with those of Inoue et al. (2004) and Mao et al. (2008b), assuming 60 vol%. Kennett et al. (1995) and Gaherty et al. (1996) report a bulk sound velocity contrast of 3 to ~ 5% at the 410 km discontinuity from seismic studies. The upper limit of 5% is quite consistent with contrast of anhydrous condition of this study, whereas the lower limit of 3% corresponds to 2.2 wt% H_2O for the current study, and 1.2 wt% H_2O for Mao et al. (2008b). On the other hand, Benz and Vidale (1993) and Nolet et al. (1994) reported 4.6% contrast from seismological studies, which corresponds to about 1.1 wt% H_2O for the current study, 1.5 wt% H_2O for Inoue et al. (2004), and about 0.4 wt% H_2O for Mao et al. (2008b). Although different studies give different water contents (ranges) for the 410 km discontinuity, all are qualitatively consistent with significant water contents in upper mantle and transition zone, whereas the bulk sound velocity contrast at anhydrous conditions would be larger than those indicated by seismic studies.

ACKNOWLEDGMENTS

The sample synthesis work was supported by U.S. National Science Foundation Grant EAR 07-11165, and single-crystal X-ray diffraction measurements were conducted at Mineral Physics and Crystallography Lab, in Geological Sciences, University of Colorado at Boulder.

REFERENCES CITED

Anderson, D.L. (2007) New Theory of the Earth. Cambridge University Press, U.K.

Benz, H.M. and Vidale, J.E. (1993) Sharpness of upper-mantle discontinuities determined from high-frequency reflections. Nature, 365, 147–150.

Chopelas, A. (1991) Thermal properties of β-Mg_2SiO_4 at mantle pressures derived from vibrational spectroscopy: Implications for the mantle at 410 km depth. Journal of Geophysical Research, 96, 11817–11829.

Couvy, H., Chen, J., and Drozd, V. (2010) Compressibility of nanocrystalline forsterite. Physics and Chemistry of Minerals, 37, 343–351.

Cromer, D.T. and Mann, J. (1968) X-ray scattering factors computed from numerical Hartree-Fock wave functions. Acta Crystallographica, A24, 321–325.

Deon, F., Koch-Müller, M., Rhede, D., Gottschalk, M., Wirth, R., and Thomas, S-M. (2010) Location and quantification of hydroxyl in wadsleyite: New insights. American Mineralogist, 95, 312–322.

Dziewonski, A.M. and Anderson, D.L. (1981) Preliminary reference Earth model. Physics of the Earth and Planetary Interiors, 25, 297–356.

Downs, R.T., Bartelmehs, K.L., Gibbs, G.V., and Boisen, M.B. (1993) Interactive software for calculating and displaying X-ray or neutron powder diffractometer patterns of crystalline materials. American Mineralogist, 78, 1104–1107.

Farrugia, L.J. (1999) WinGX software package. Journal of Applied Crystallography, 32, 837–838.

Gaherty, J.B., Jordan, T.H., and Gee, L.S. (1996) Seismic structure of the upper mantle in a central Pacific corridor. Journal of Geophysical Research, 101, 22291–22309.

Holl, C.M., Smyth, J.R., Jacobsen, S.D., and Frost, D.J. (2008) Effects of hydration on the structure and compressibility of wadsleyite, β-(Mg_2SiO_4). American Mineralogist, 93, 598–607.

Inoue, T., Tanimoto, Y., Irifune, T., Suzuki, T., Fukui, H., and Ohtaka, O. (2004) Thermal expansion of wadsleyite, ringwoodite, hydrous wadsleyite and hydrous ringwoodite. Physics of the Earth and Planetary Interiors, 143–144, 279–290.

Jacobsen, S.D., Demouchy, S., Frost, D.J., Boffa-Ballaran, T., and Kung, J. (2005) A systematic study of OH in hydrous wadsleyite from polarized FTIR spectroscopy and single-crystal X-ray diffraction: Oxygen sites for hydrogen storage in the Earth's interior. American Mineralogist, 90, 61–70.

Kennett, B.L.N., Engdahl, E.R., and Buland, R. (1995) Constraints on seismic velocities in the Earth from travel-time. Geophysical Journal International, 122, 108–124.

Kudoh, Y. and Inoue, T. (1999) Mg-vacant structural modules and dilution of the symmetry of hydrous wadsleyite, β-$Mg_{2-X}SiH_{2X}O_4$ with $0.00 \le X \le 0.25$. Physics and Chemistry of Minerals, 26, 382–388.

Li, B., Liebermann, R.C., and Weidner, D.J. (1998) Elastic moduli of wadsleyite (β-Mg_2SiO_4) to 7 Gigapascals and 873 Kelvin. Science, 281, 675–677.

Mao, Z., Jacobsen, S.D., Jiang, F., Smyth, J.R., Holl, C.M., and Duffy, T.S. (2008a) Single-crystal elasticity of wadsleyities, β-Mg_2SiO_4, containing 0.37−1.66 wt% H_2O. Earth and Planetary Science Letters, 266, 78–89.

——— (2008b) Elasticity of hydrous wadsleyite to 12 GPa: Implications for Earth's transition zone. Geophysical Research Letters, 35, L21305, DOI: 10.1029/2008Ge035618.

Nolet, G., Grand, S.P., and Kennett, B.L. (1994) Seismic heterogeneity in the upper mantle. Journal of Geophysical Research, 99, 23753–23766.

Ringwood, A.E. (1966) The chemical composition and origin of the earth. In P.M. Hurley, Ed., Advances in Earth Science, p. 287–356. M.I.T. Press, Cambridge, Massachusetts.

Sheldrick, G.M. (1997) SHELXL97, Release 97-2. Program for the refinement of crystal structures. University of Göttingen, Germany.

Smyth, J.R. (1987) β-Mg_2SiO_4: a potential host for water in the mantle? American Mineralogist, 72, 1051–1055.

——— (1994) A crystallographic model for hydrous wadsleyite: An ocean the Earth's interior? American Mineralogist, 79, 1021–1025.

Smyth, J.R., Frost, D.J., Nestola, F., Holl, C.M., and Bromiley, G. (2006) Olivine hydration in the deep upper mantle: effects of temperature and silica activity. Geophysical. Research Letters, 33, L15301.

Smyth, J.R., Kawamoto, T., Jacobsen, S.D., Swope, R.J., Hervig, R.L., and Holloway, J.R. (1997) Crystal structure of momoclinic hydrous wadsleyite. American Mineralogist, 82, 270–275.

Stebbins, J.F., Panero, W.R., Smyth, J.R., and Frost, D.J. (2009a) Forsterite, wadsleyite and ringwoodite: ^{29}Si NMR constraints on structural disorder and effects of paramagnetic impurity ions. American Mineralogist, 94, 626–629.

——— (2009b) Forsterite, hydrous and anhydrous wadsleyite and ringwoodite (Mg_2SiO_4): ^{29}Si NMR results for chemical shift anisotropy, spin-lattice relaxation, and mechanism of hydration. American Mineralogist, 94, 905–915.

Tokonami, M. (1965) Atomic scattering factor for O^{2-}. Acta Crystallographica, 19, 486.

Ye, Y., Schwering, R.A., and Smyth, J.R. (2009) Effects of hydration on thermal expansion of forsterite, wadsleyite, and ringwoodite at ambient pressure. American Mineralogist, 94, 899–904.

Ye, Y., Smyth, J.R., Hushur, A., Manghnani, M.H., Lonappan, D., Dera, P., and Frost, D.J. (2010) Crystal structure of hydrous wadsleyite with 2.8% H_2O and compressibility to 60 GPa. American Mineralogist, 95, 1765–1772.

MANUSCRIPT RECEIVED APRIL 4, 2011
MANUSCRIPT ACCEPTED JULY 25, 2011
MANUSCRIPT HANDLED BY ALEXANDRA FRIEDRICH